SUPPLEMENTAL MATERIAL

SUPPORTING METHODS

Model equations

The full equations for APD restitution and Ca cycling are given below, originally from Qu et al. [33], except for the APD restitution function, which comprise the full model including the equations provided in the main text. Parameter values are given in Table S1. Plots of key equation relationships are shown in Fig. S1.

The APD restitution function is given by

$$f(d_n) = \begin{cases} a_0\left[1 - \exp((d_n - d_0)/\tau_0)\right], & \text{if } d_n \geq d_{min} \\ 0, & \text{otherwise} \end{cases} \tag{S1}$$

The SR Ca release function that describes the restitution properties is given by

$$q(d_n) = 1 - \sigma_q \exp(-d_n/\tau_q), \tag{S2}$$

and the function that describes the SR Ca load-dependence is given by

$$g(l_n) = l_n \left[1 - \frac{1-\alpha}{1+\exp((l_n - l_c)/\beta)}\right]. \tag{S3}$$

The SR Ca uptake function that describe the dependence on the stimulus period is given by

$$u(t_{n+1}) = 1 - \rho \exp(-t_{n+1}/\tau_u), \tag{S4}$$

and the function that describes the dependence on peak intracellular Ca is given by

$$h(c^p_{n+1}) = c^p_{n+1}\left[1 - \frac{1}{1+\exp((c^p_{n+1} - c_0)/\theta)}\right]. \tag{S5}$$

The steady-state total Ca concentration is given by

$$c(t_{n+1}) = c_0[1 + \varepsilon \exp(-t_{n+1}/\tau_c)]. \tag{S6}$$

SUPPORTING TABLE

Parameter	Definition	Units	NSR Value	CHF Value
a_0	APD restitution parameter	ms	275.9279	372.3244
d_0	APD restitution parameter	ms	437.7602	535.1088
τ_0	APD restitution parameter	ms	474.0194	803.6337
d_{min}	APD restitution parameter	ms	10	10
σ_q	SR Ca release parameter	-	0.5	0.5
τ_q	SR Ca release parameter	ms	160*	160*
α	SR Ca release parameter	-	0.036	0.036
l_c	SR Ca release parameter	μM	93.5	93.5
β	SR Ca release parameter	μM	14.6463	13.4016
ν	SR Ca uptake parameter	-	0.4787	0.4948
ρ	SR Ca uptake parameter	-	0.15	0.15
τ_u	SR Ca uptake parameter	ms	400*	400*
c_0	SR Ca uptake parameter	μM	28	28
θ	SR Ca uptake parameter	μM	20	20
γ	Ca-to-APD coupling parameter	μM^{-1}	10^{-3}	10^{-3}
ε	Ca accumulation parameter	-	2	2
τ_c	Ca accumulation parameter	ms	600*	600*
κ	Ca accumulation parameter	-	0.1	0.1
η	APD-to-Ca coupling parameter	μM/ms	0.1	0.1
λ	SR Ca release parameter	-	2.9864	3.0413
δ	SR Ca leak parameter	-	0	0.5464

Table S1. Model parameters. All parameters pertaining to the APD and Ca dynamics for NSR and CHF. * denotes parameters scaled by a factor of 2 to account for differences in heart rates betweem humans and small mammals.

SUPPORTING FIGURES

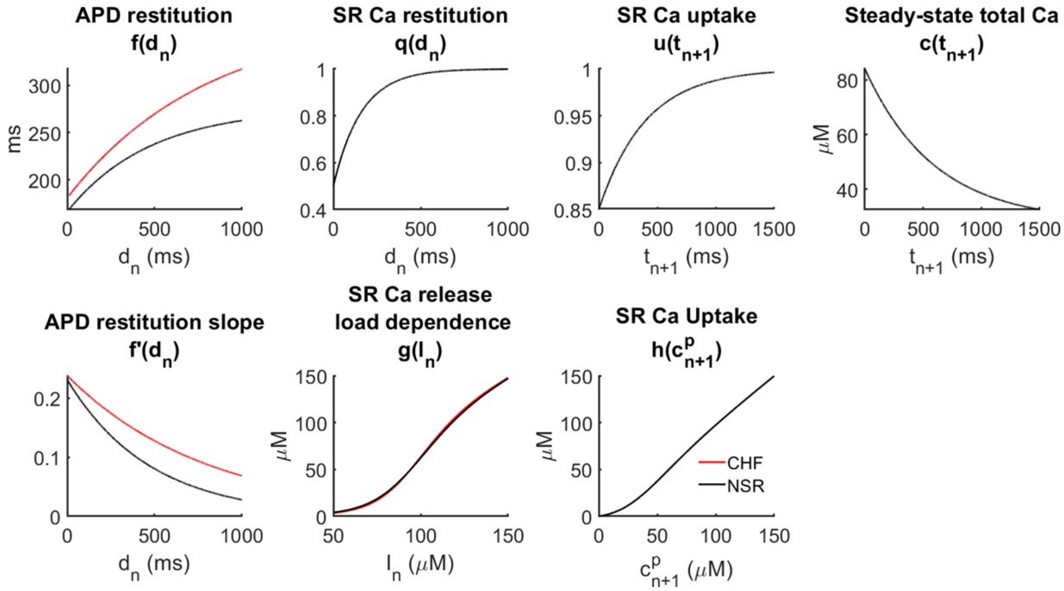

Figure S1. Discrete-time map model functions. Plots of the discrete-time map model functions and the APD restitution curve for NSR (black) and CHF (red).

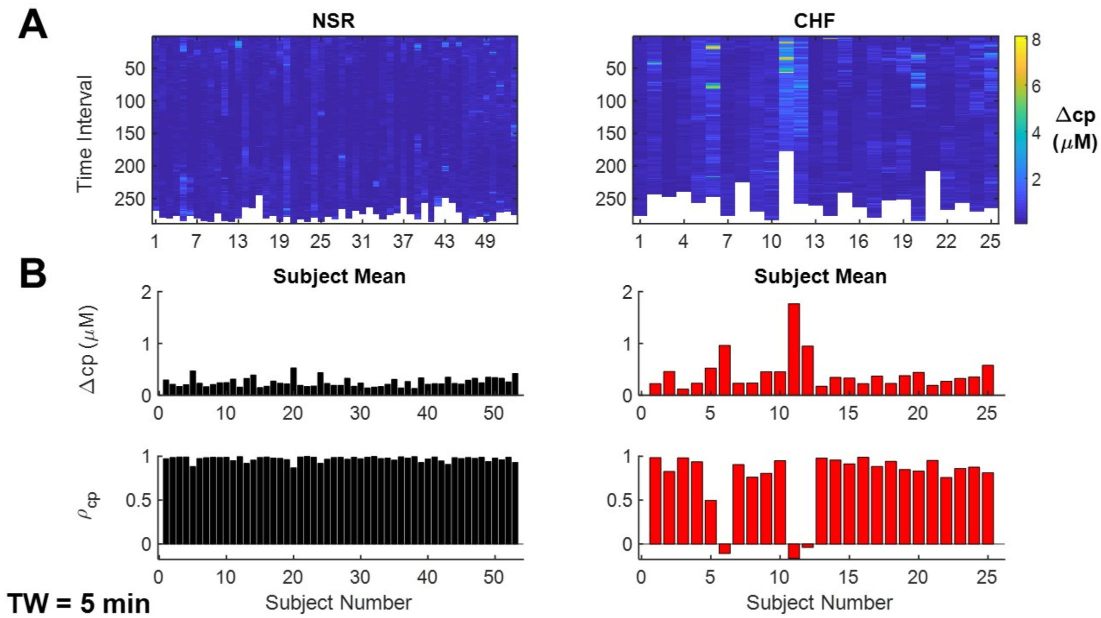

Figure S2. Peak Ca alternans formation is more prevalent in CHF. (A) Δc^p is shown for each 5 minute segment of every 24 hour RR sequence in both populations. (B) The temporal average of Δc^p and ρ_{c^p} are depicted for each subject in the NSR (black) and CHF (red) populations. TW = 5 minutes.

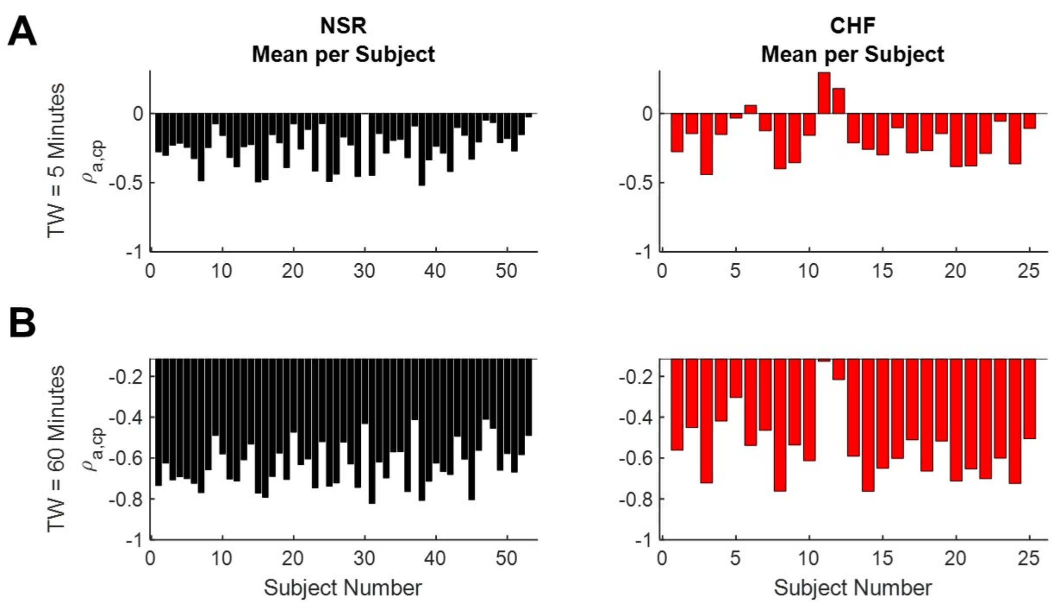

Figure S3. APD and peak Ca tend to be negatively correlated in NSR and CHF. Each subject's mean ρ_{a,c^p} is shown for a short (TW = 5 minutes, A) and long (TW = 60 minutes, B) time window.

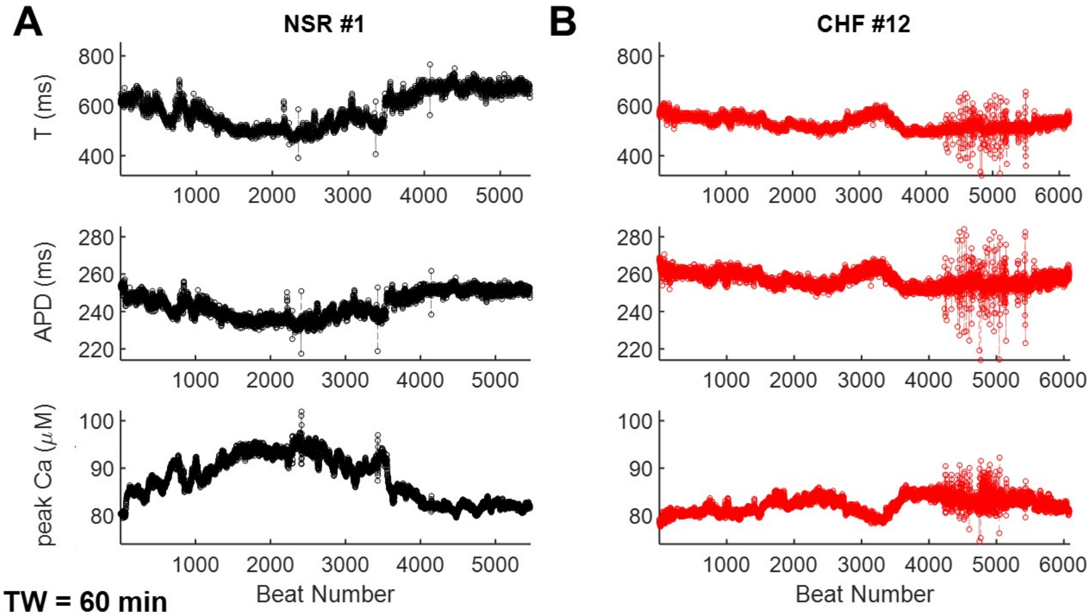

Figure S4. At a longer duration, the trends in NSR electrical activity are consistent with the shorter simulation. In CHF, there is less overall variability though there are periods with similar properties to the 5 minute simulation. Traces of a 60 minute pacing sequence (top) and the corresponding APD (middle) and peak Ca (bottom) beat-to-beat values are depicted from (A) NSR #1 and (B) CHF #12. TW = 60 minutes.

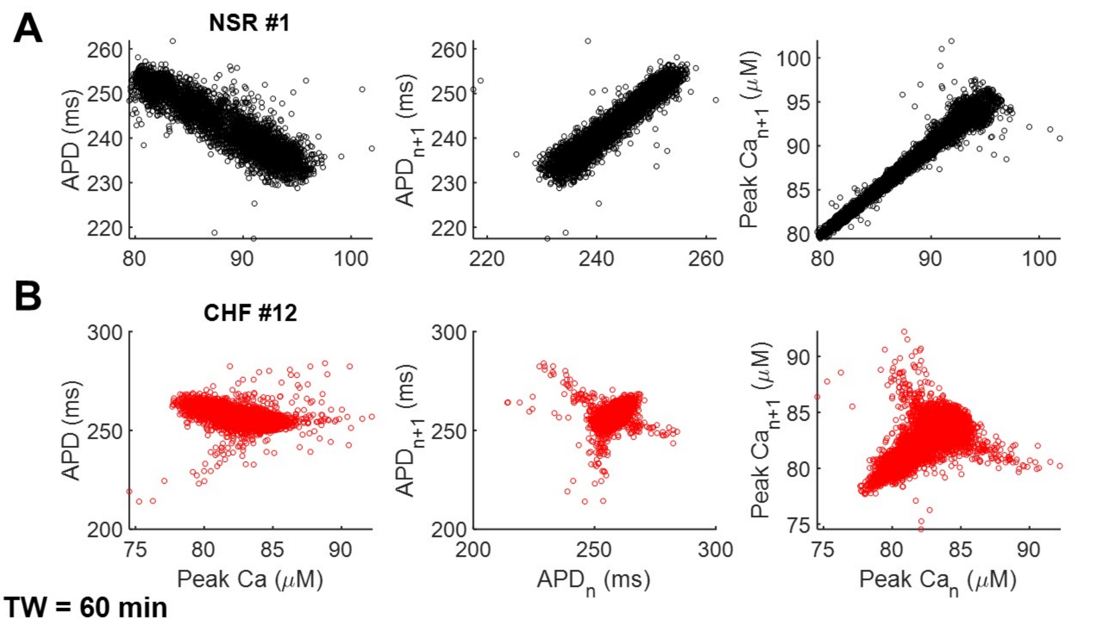

Figure S5. The relationship between APD and peak Ca and the correlations between consecutive APD and peak Ca values are consistent at a longer TW of 1 hour in NSR and CHF. Scatter plots of APD vs. peak Ca (left), successive APD values (middle), and successive peak Ca values (right) are shown for the (A) NSR #1 and (B) CHF #12 simulations depicted in Fig. S4. TW = 60 minutes.

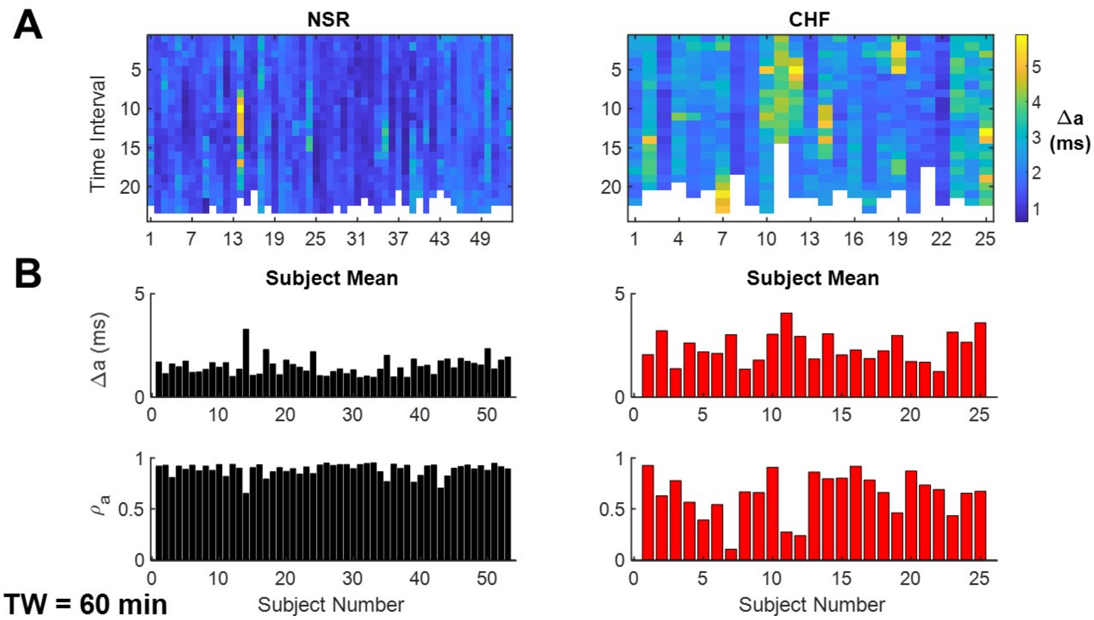

Figure S6. Consistent with shorter simulations, APD alternans formation is more likely in the CHF population. (A) Δa is shown for each one hour segment of every 24 hour RR sequence in both populations. (B) The temporal average of Δa and ρ_a are depicted for each subject in the NSR (black) and CHF (red) populations. TW = 60 minutes.

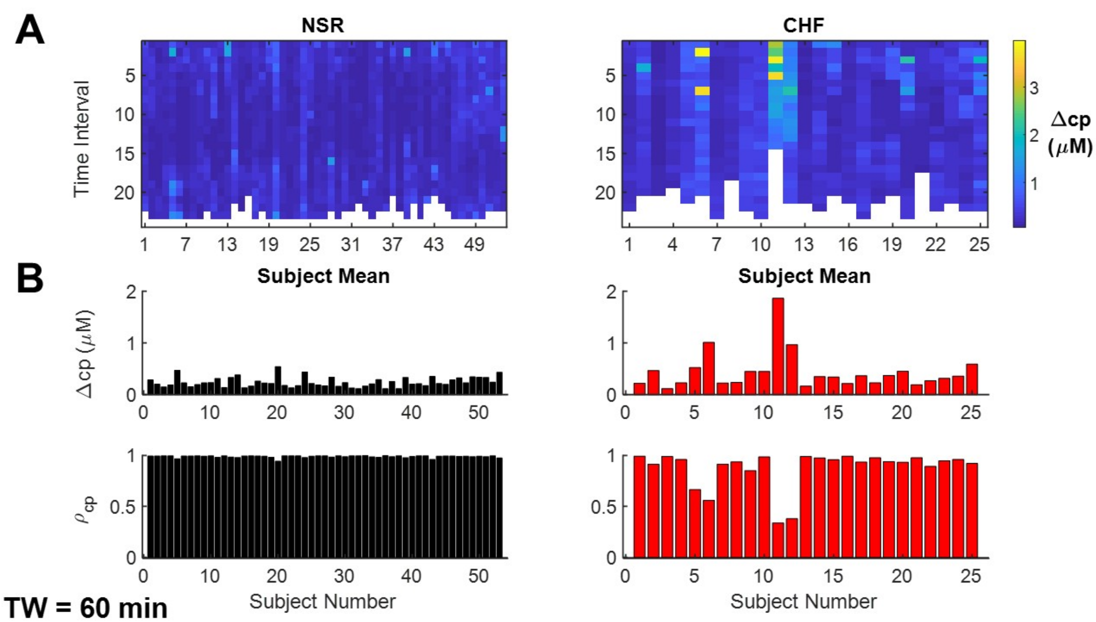

Figure S7. Similar to the 5 minute TW, peak Ca alternans formation is more prevalent in CHF. (A) Δc^p is shown for each one hour segment of every 24 hour RR sequence in both populations. (B) The temporal average of Δc^p and ρ_{c^p} are depicted for each subject in the NSR (black) and CHF (red) populations. TW = 60 minutes.

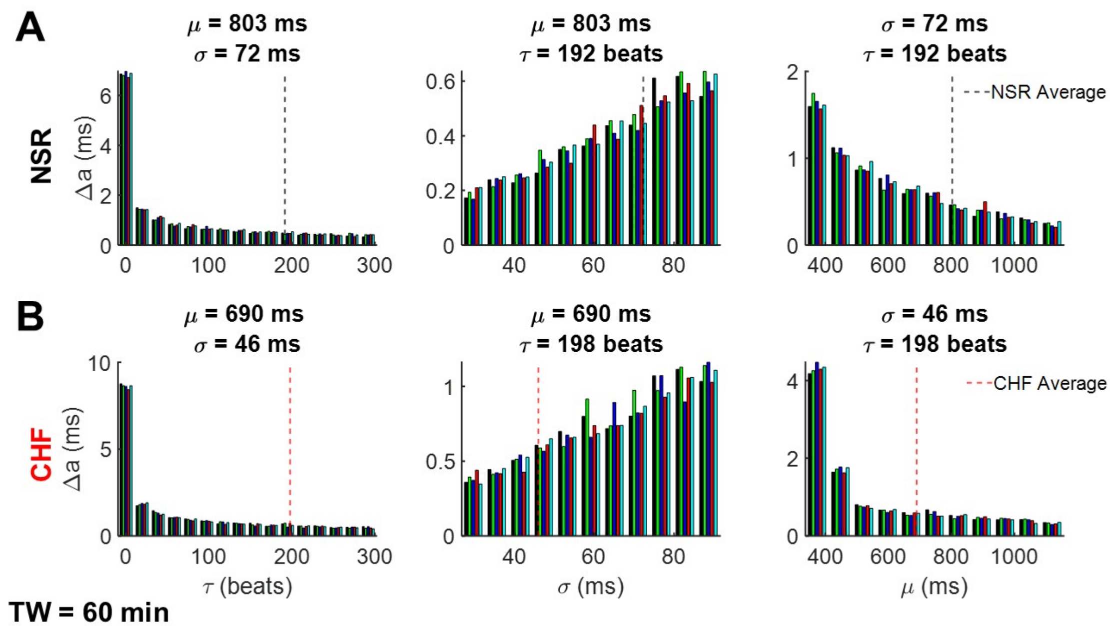

Figure S8. The influence of each statistical property at a long TW is consistent with trends seen in 5 minute simulations. Δa is shown for 5 synthetic sequences for different combinations of statistical properties, where τ (left), σ (middle), and μ (right) are broadly varied and the remaining two parameters are the population average. The third NSR and CHF average parameter value is shown in black and red, respectively. Results are shown for both the (A) NSR and (B) CHF models. TW = 60 minutes.

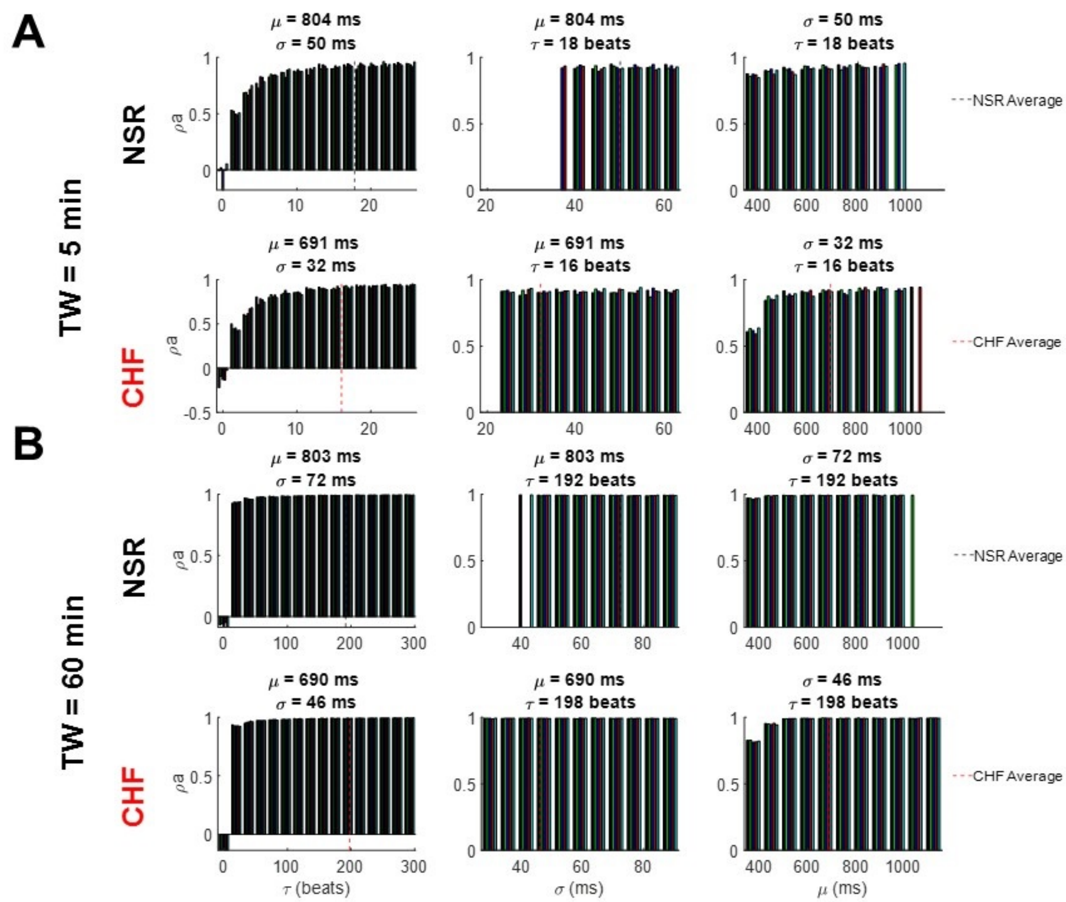

Figure S9. Increasing the autocorrelation time promotes consistency in APD. ρ_a is shown for 5 synthetic sequences for different combinations of statistical properties, where τ (left), σ (middle), and μ (right) are broadly varied and the remaining two parameters are the population average using the NSR and CHF models. The third NSR and CHF average parameter value is shown in black and red, respectively. Values are shown for TWs of (A) 5 and (B) 60 minutes.

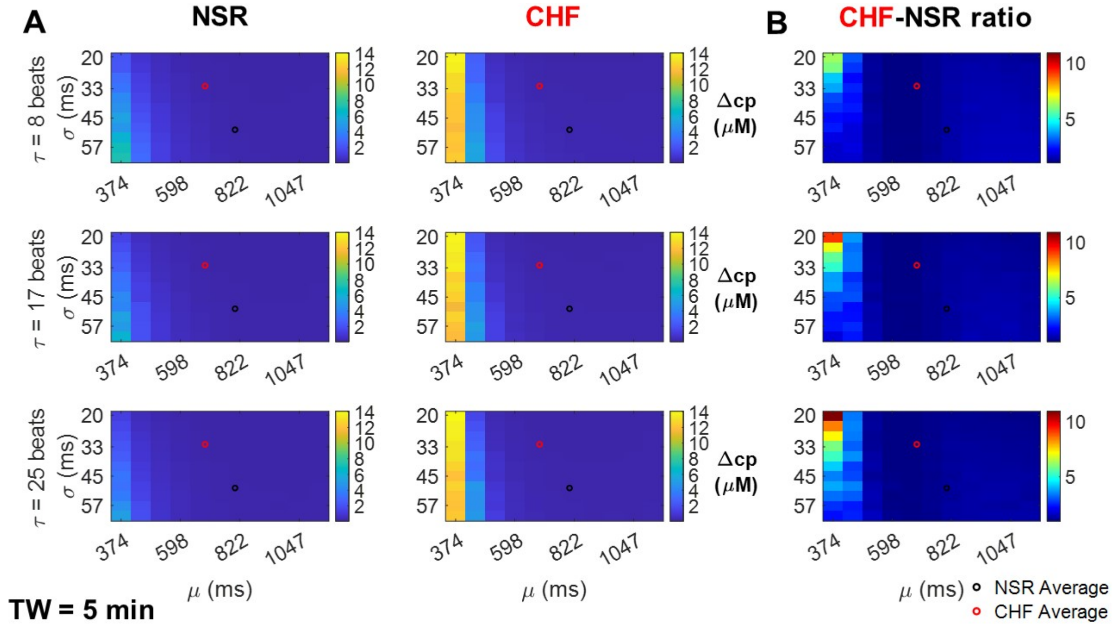

Figure S10. For a specific synthetic sequence, the CHF model leads to greater peak Ca alternations than the NSR model. The Δc^p value is plotted for different values of μ (x-axis), σ (y-axis), and τ (row) using the NSR (left) and CHF (middle) models. The average NSR and CHF μ and σ are depicted in black and red (A). The corresponding ratio of CHF to NSR $\Delta c^p$is also shown (right, B). TW = 5 minutes.

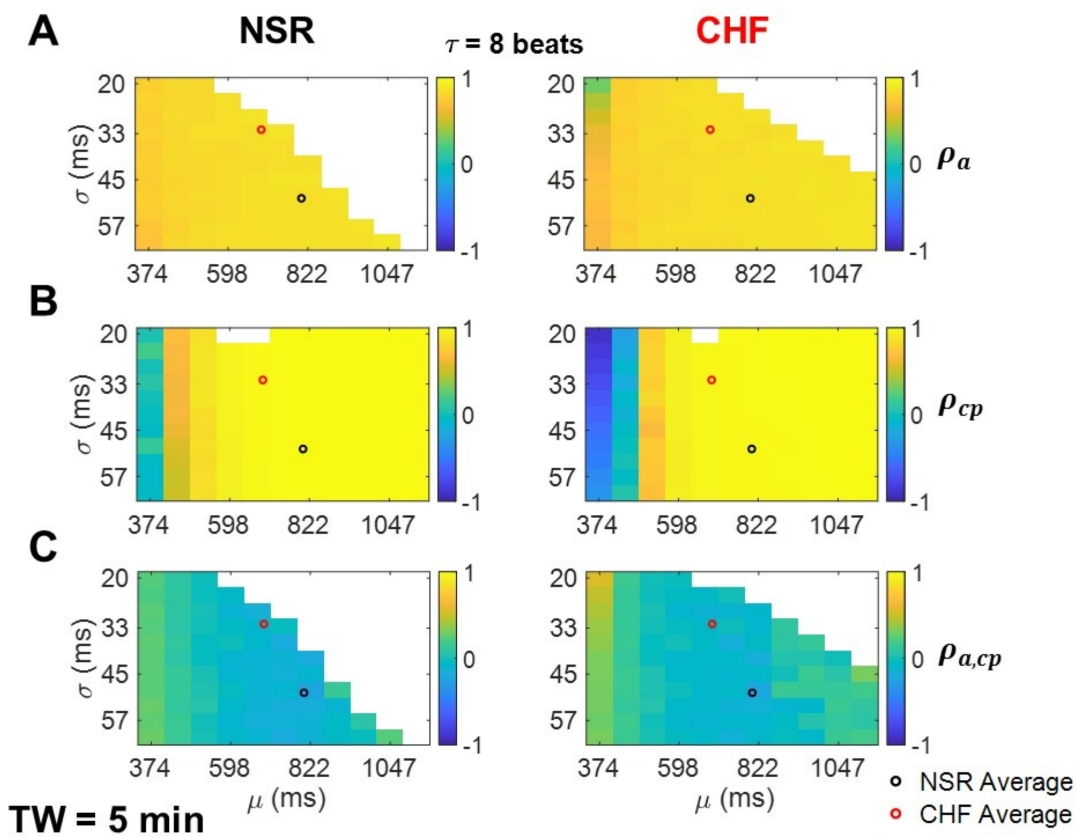

Figure S11. The ρ_a (A), ρ_{c^p} (B), and ρ_{a,c^p} (C) values are plotted for $\tau = 8$ beats and different values of μ (x-axis), and σ (y-axis) using the NSR (left) and CHF (right) models. The average NSR and CHF μ and σ are depicted in black and red. TW = 5 minutes.

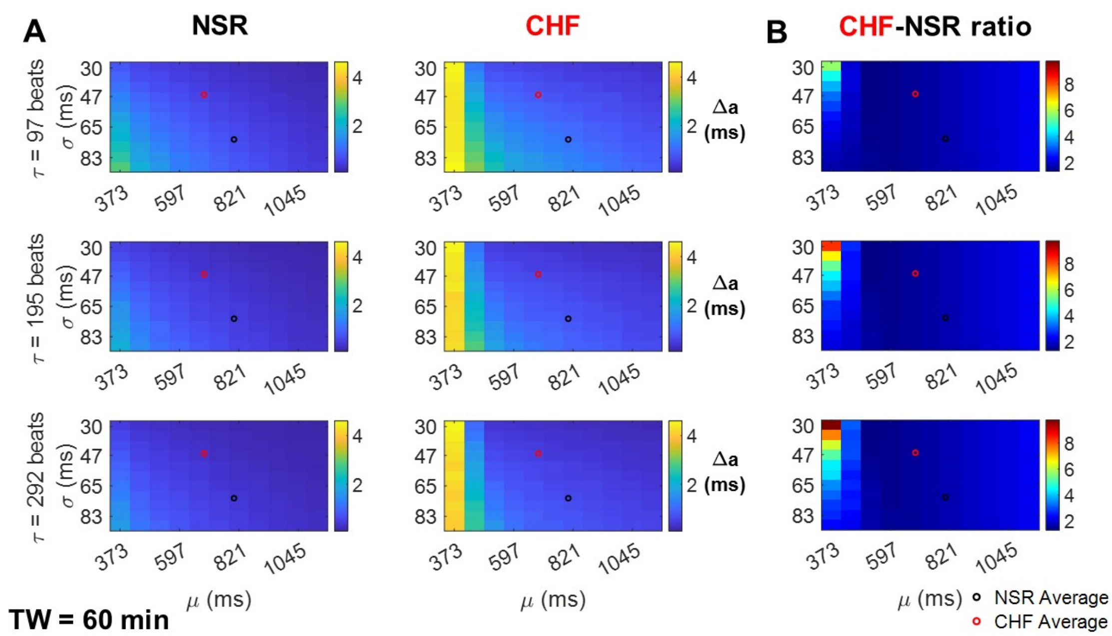

Figure S12. The effect of model parameters on Δa are similar on both a short and long time scale. (A) The Δa value is plotted for different values of μ (x-axis), σ (y-axis), and τ (row) using the NSR (left) and CHF (middle) models. The average NSR and CHF μ and σ are depicted in black and red. (B) The corresponding ratio of CHF to NSR Δa is also shown (right). TW = 60 minutes.